SEMARAK ILMU PUBLISHING

Journal of Advanced Research in Fluid Mechanics and Thermal Sciences

Journal homepage:
https://semarakilmu.com.my/journals/index.php/fluid_mechanics_thermal_sciences/index
ISSN: 2289-7879

Numerical Study of Aerodynamic Characteristics of a Pointed Plate of Variable Elongation in Subsonic and Supersonic Gas Flow

Serhii Alekseyenko[1], Andrii Dreus[2,*], Mykola Dron[3], Olexandr Brazaluk[2]

[1] Mechatronics Department, Physical and Technical Faculty, Oles Honchar Dnipro National University, Dnipro, 49010, Ukraine
[2] Department of Fluid Mechanics and Energy & Mass Transfer, Faculty of Mechanics and Mathematics, Oles Honchar Dnipro National University, Dnipro, 49010, Ukraine
[3] Department of Launch Vehicle, Physical and Technical Faculty, Oles Honchar Dnipro National University, Dnipro, 49010, Ukraine

ARTICLE INFO

Article history:
Received 25 February 2022
Received in revised form 17 May 2022
Accepted 20 May 2022
Available online 18 June 2022

Keywords:
Computational aerodynamics; flow acting on a thick plate; variable geometry; drag coefficient

ABSTRACT

This study shows a thick plate, pointed on both sides, of variable elongation under action of subsonic and supersonic air flows. The relevance of the work is driven by the development of new aircraft that change their geometry during the flight, in particular, aircraft that change the relative elongation during the flight. The aim of this work is to determine the aerodynamic fields around the pointed plate, taking into account its variable elongation, and to determine the effect of variable elongation on the drag coefficient of the plate. Numerical simulation was used as a research tool. Mathematical modeling is based on Reynolds-averaged Navier-Stokes equations. The original software was used for the analysis; the computational algorithm is based on the finite volume method. The mathematical model and algorithm of numerical computation of subsonic and supersonic air flow acting on a pointed plate are presented. A pattern of gas flow acting on the plate is obtained at zero angle of attack for Mach numbers from 0,6 to 4. The dependence of the plate drag coefficient on Mach number and relative elongation is obtained. It is established that for a thick pointed plate the drag coefficient significantly depends on the elongation for both sound and supersonic flow. As a result of numerical experiments, the anomalous behavior of the drag coefficient in the transonic area at large elongations was found. It is shown that the decrease in elongation leads to an increase in the drag coefficient of the plate, which affects the aerodynamic characteristics of the aircraft of variable elongation.

1. Introduction

The tasks of infinite wedges or plates in subsonic and supersonic air flow conditions are classic in computational aerodynamics [1]. At the same time, the study of such problems remains relevant due to the intensive development of new subsonic and supersonic aircraft that use structural elements of similar geometric shapes. Such elements include load-bearing surfaces, high-lift devices, fuselages and aircraft bodies, control and stabilization systems, etc. During the study of aerodynamic

* *Corresponding author.*
E-mail address: dreus.andrii@gmail.com

https://doi.org/10.37934/arfmts.96.2.8897

characteristics many of these objects are often modeled as infinite aerodynamic profiles, plates, wedges, cones, and so on.

It is possible to indicate a number of relevant and practically important tasks where such models are used, such as in the studies by Khan *et al.,* [2], Aabid *et al.,* [3], Traub [4], and Yusof *et al.,* [5]. In particular, in computational aerodynamics, pointed wedges are used to generate shock waves [6]. The same problems are also of interest for calculation of hypersonic air intakes and subsonic diffusers [7,8]. It should be noted that modern aircraft and structural elements can change its aerodynamic configuration in flight due construction features, or physical phenomena, that results in changes in aerodynamic characteristics [9-11]. Likewise, a number of tasks have recently emerged, in which the aircraft change the elongation, that must be taken into account when designing a flight program [12,13]. Similar problems arise when estimating aerodynamic and thermal loads on fragments of space debris discharged from low Earth orbits into the Earth's atmosphere [14,15]. Thus, there is a request to study the aerodynamic characteristics of bodies of variable geometry, both in subsonic and supersonic gas flows.

Among the known works in this area, the work of Petrov [16] should be highlighted. This work provides experimental data on aerodynamic characteristics of individual structural elements of aircraft of different geometries and sizes. However, the presented results are not universal and do not cover all the possible options. In connection with the above-mentioned tasks, one of the geometric shapes of practical interest is the infinite plate pointed on both sides, which is surrounded by gas flow. The aim of this work is to determine the aerodynamic fields around such a plate, taking into account the change in its elongation, and to determine the effect of variable elongation on the aerodynamic characteristics - the drag coefficient of the element. The solution of this task is performed by mathematical modeling and computational experiment.

2. Methodology

2.1 Mathematical Statement of the Problem

A smooth plate, the pointed front of which is in conditions of non-heat-conducting gas flow, is considered at zero angle of attack (Figure 1).

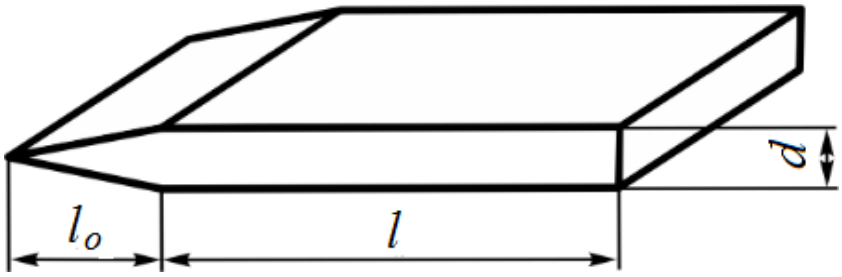

Fig. 1. The scheme of a thick pointed plate

The flow rate varies from subsonic to supersonic, respectively, and Mach numbers vary from M = 0,6 to M = 4. We will also consider plates of different elongation of the smooth part $l/d = 6, 10, 15$, where of the wedge-shaped part to smooth part $l_o/d = 2{,}57$. Such dimensions correlate with the design parameters of rockets of variable elongation that are being designed [17]. Assume that there is no effect of heat transfer processes on the velocity and pressure field around the plate. Modeling of aerodynamic processes is performed in a two-dimensional formulation in an arbitrary coordinate

system (ξ, η) based on Reynolds-averaged Navier-Stokes equations for compressible fluids, which can be written in vector form as follows

$$\frac{\partial \mathbf{q}}{\partial t}+\frac{\partial \mathbf{E}}{\partial \xi}+\frac{\partial \mathbf{F}}{\partial \eta}=\frac{1}{\mathrm{Re}}\left(\frac{\partial \hat{\mathbf{E}}}{\partial \xi}+\frac{\partial \hat{\mathbf{F}}}{\partial \eta}\right), \tag{1}$$

$$\mathbf{q}=\begin{bmatrix}\rho\\ \rho u\\ \rho v\\ e\end{bmatrix}, \qquad \mathbf{E}=\frac{1}{J}\begin{bmatrix}\rho U\\ \rho u U+\xi_x p\\ \rho v U+\xi_y p\\ (e+p)U\end{bmatrix}, \quad \mathbf{F}=\frac{1}{J}\begin{bmatrix}\rho V\\ \rho u V+\eta_x p\\ \rho v V+\eta_y p\\ (e+p)V\end{bmatrix}, \tag{2}$$

$$\hat{\mathbf{E}}=\frac{1}{J}\begin{bmatrix}0\\ \xi_x\tau_{xx}+\xi_y\tau_{xy}\\ \xi_x\tau_{yx}+\xi_y\tau_{yy}\\ \xi_x\beta_x+\xi_y\beta_y\end{bmatrix}, \qquad \hat{\mathbf{F}}=\frac{1}{J}\begin{bmatrix}0\\ \eta_x\tau_{xx}+\eta_y\tau_{xy}\\ \eta_x\tau_{yx}+\eta_y\tau_{yy}\\ \eta_x\beta_x+\eta_y\beta_y\end{bmatrix}, \tag{3}$$

$$U=\xi_x u+\xi_y v, \quad V=\eta_x u+\eta_y v, \tag{4}$$

$$\tau_{xx}=\frac{2\mu}{3}\left[2(\xi_x u_\xi+\eta_x u_\eta)-(\xi_y v_\xi+\eta_y v_\eta)\right], \tag{5}$$

$$\tau_{yy}=\frac{2\mu}{3}\left[2(\xi_y u_\xi+\eta_y u_\eta)-(\xi_x v_\xi+\eta_x v_\eta)\right], \tag{6}$$

$$\tau_{xy}=\tau_{yx}=\mu\left[(\xi_y u_\xi+\eta_y u_\eta)-(\xi_x v_\xi+\eta_x v_\eta)\right], \tag{7}$$

$$\beta_x=u\tau_{xx}+v\tau_{xy}+\frac{1}{\gamma-1}\left(\frac{\mu_l}{\mathrm{Pr}_l}+\frac{\mu_t}{\mathrm{Pr}_t}\right)\left(\xi_x\frac{\partial a^2}{\partial \xi}+\eta_x\frac{\partial a^2}{\partial \eta}\right), \tag{8}$$

$$\beta_y=u\tau_{yx}+v\tau_{yy}+\frac{1}{\gamma-1}\left(\frac{\mu_l}{\mathrm{Pr}_l}+\frac{\mu_t}{\mathrm{Pr}_t}\right)\left(\xi_y\frac{\partial a^2}{\partial \xi}+\eta_y\frac{\partial a^2}{\partial \eta}\right), \tag{9}$$

where here x, y - axes of Cartesian coordinate system; ρ – density; a – sound speed; u, v – components of the velocity vector in the x, y directions; p – pressure; e – total energy per unit of gas volume; Pr_l – molecular Prandtl number; $\mathrm{Pr}_t=0{,}9$ – turbulent Prandtl number, $\mu=\mu_l+\mu_t$ – dynamic coefficient of "effective" viscosity; μ_l – dynamic coefficient of molecular viscosity; μ_t – dynamic coefficient of turbulent viscosity; γ – gas adiabatic index.

The metric coefficients and Jacobian of coordinates transformation included in Eq. (1) to Eq. (9), are determined from the expressions

$$\xi_x = Jy_\eta,\ \xi_y = -Jx_\eta,\ \eta_x = -Jy_\xi,\ \eta_y = Jx_\xi,$$

$$J = \frac{\partial(\xi,\eta)}{\partial(x,y)} = \begin{vmatrix} \xi_x & \xi_y \\ \eta_x & \eta_y \end{vmatrix}.$$

To close the system (1) and to determine the coefficient of turbulent viscosity. The different turbulence models were discussed in a study by Khan *et al.,* [18]. The Spalart-Allmaras model was used herein, which was well-proven at the analysis of problems of external flow around bodies and is described in detail in the study by Spalart and Allmaras [19].

To numerically study the flow around the plate, a design O-mesh was made according to algebraic formulas at the design area between the body surface and the distant boundary. The dimensions of the mesh were fined near the surface of the body, see Figure 2.

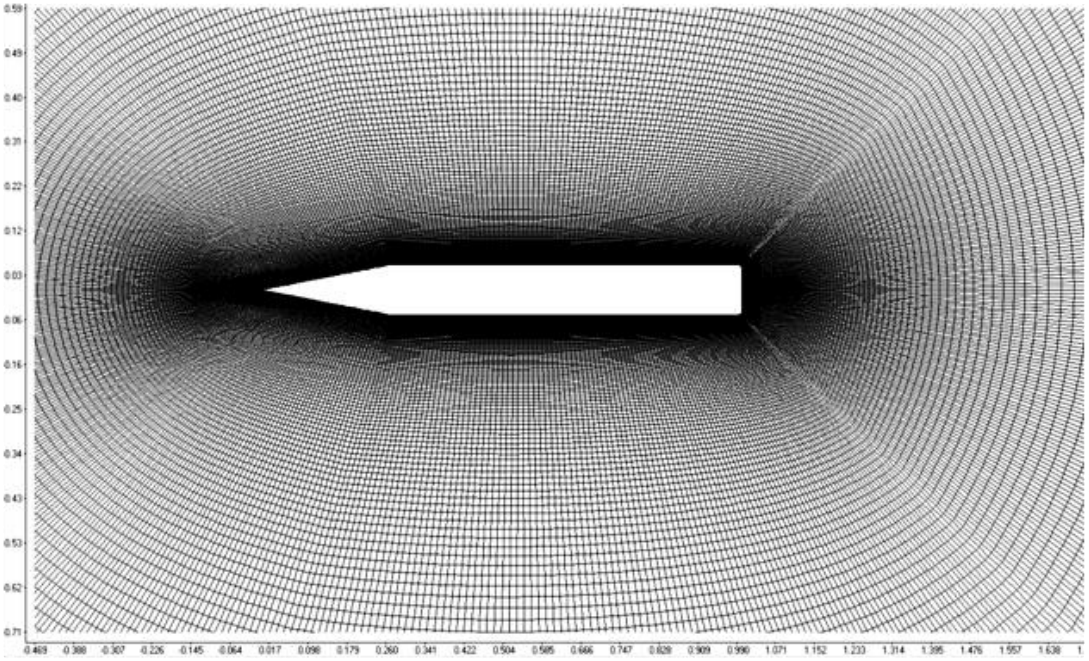

Fig. 2. The mesh scheme of a thick pointed plate

Boundary conditions, which are formulated based on the stated below, are added to the system. Adhesion conditions $\mathbf{v} = 0$ are set on the surface of the plate. Correct setting of boundary conditions at the distant boundary of the area is more difficult [20]. Boundary conditions vary for the area boundaries where the gas flow goes in and out. One-dimensional Euler equations were used to calculate the normal velocity component at the distant boundary, the characteristics of which are not difficult to determine. Thus, the connection between the modulus of the velocity vector q and the sound speed a can be expressed using Riemann invariants.

$$0.5q_b - \frac{a}{\gamma - 1} = 0.5q_\infty - \frac{a_\infty}{\gamma - 1},$$

where the index b refers to the area boundary, index ∞ refers to the undisturbed flow. The values of the tangential component of the velocity vector were recorded at the upper and lower boundaries of the area.

2.2 Numerical Schema

Discretization of the system of initial Navier-Stokes Eq. (1) was performed using the finite volume method for curvilinear coordinates

$$\frac{3\Delta\mathbf{q}^{n}-\Delta\mathbf{q}^{n-1}}{2\Delta t}+\mathbf{R}^{n+1}=0, \tag{10}$$

where n – is the number of the time layer

$$\Delta\mathbf{q}^{n}=\mathbf{q}^{n+1}-\mathbf{q}^{n};\ \Delta\mathbf{q}^{n-1}=\mathbf{q}^{n}-\mathbf{q}^{n-1},$$
$$\mathbf{R}^{n+1}=\frac{\mathbf{E}_{i+1/2}^{n+1}-\mathbf{E}_{i-1/2}^{n+1}}{\Delta\xi}+\frac{\mathbf{F}_{i+1/2}^{n+1}-\mathbf{F}_{i-1/2}^{n+1}}{\Delta\eta}-\frac{1}{\mathrm{Re}}\left(\frac{\hat{\mathbf{E}}_{i+1/2}^{n+1}-\hat{\mathbf{E}}_{i-1/2}^{n+1}}{\Delta\xi}+\frac{\hat{\mathbf{F}}_{j+1/2}^{n+1}-\hat{\mathbf{F}}_{j-1/2}^{n+1}}{\Delta\eta}\right),$$

To calculate the convective terms, the Roe scheme is used, which shows a satisfactory computational accuracy for such tasks [21]. According to this scheme the flows that go through the cell face $i+1/2$ of the finite volume are determined by

$$\mathbf{E}_{i+1/2}=\frac{1}{2}\left(\mathbf{E}(q_L)+\mathbf{E}(q_R)-|\mathbf{A}|(q_R-q_L)\right),$$

where q_L, q_R – are flow parameters to the left and to the right of the cell face, respectively.

To ensure the second order of accuracy in space, the following extrapolation was used

$$q_L=q_i+\psi(\Delta q_{i-1/2},\Delta q_{i+3/2})),$$

$$q_R=q_i-\psi(\Delta q_{i-1/2},\Delta q_{i+3/2})),$$

where ψ – is a flow limiter, which is a function of the parameter differences at neighboring points

$$\psi=\frac{\Delta q_{i-1/2},+\Delta q_{i+3/2}}{4}\left(1-\left(\frac{\Delta q_{i-1/2}-\Delta q_{i+3/2}}{|\Delta q_{i-1/2}|+|\Delta q_{i+3/2}|+\varepsilon}\right)^2\right),\ \varepsilon=10^{-3}.$$

In formula above, $\mathbf{A}$ is the Jacobi matrix of convective flows calculated from the averaged parameters

$$\widetilde{\rho}=\sqrt{\rho_L\rho_R},$$
$$\widetilde{u}=\frac{u_L\sqrt{\rho_L}+u_R\sqrt{\rho_R}}{\sqrt{\rho_L}+\sqrt{\rho_R}},$$
$$\widetilde{v}=\frac{v_L\sqrt{\rho_L}+v_R\sqrt{\rho_R}}{\sqrt{\rho_L}+\sqrt{\rho_R}}$$

$$, \widetilde{h} = \frac{h_L\sqrt{\rho_L} + h_R\sqrt{\rho_R}}{\sqrt{\rho_L} + \sqrt{\rho_R}},$$
$$\widetilde{a}^2 = (\gamma - 1)[\widetilde{h} - 0.5 \cdot (\widetilde{u}^2 + \widetilde{v}^2)],$$

where $h = \frac{a^2}{\gamma - 1} + 0.5 \cdot (\widetilde{u}^2 + \widetilde{v}^2)$ is the enthalpy.

The viscous terms in Eq. (10) were approximated by a three-point template with the second order of accuracy. When constructing an implicit algorithm, a discrete analogue of the original Navier-Stokes equations is written with respect to the unknown increment of variables $\Delta\mathbf{q}^n$ at a new time layer $n+1$

$$\Delta\mathbf{q}^n + \frac{2}{3}\Delta t\mathbf{R}^{n+1} = \frac{1}{3}\Delta\mathbf{q}^{n-1}.$$

The residual vector $\mathbf{R}^{n+1}$ is linearized with respect to the time layer n using second-order Taylor series $O(\Delta q^n)^2$

$$\mathbf{R}^{n+1} = \mathbf{R}^n + \left(\frac{\partial\mathbf{R}}{\partial\mathbf{q}}\right)^n \Delta\mathbf{q}^n.$$

After substituting the relations on the left side of the equations, an implicit operator appears

$$\left(I + \frac{2}{3}\Delta t\frac{\partial\mathbf{R}}{\partial\mathbf{q}}\right)^n \Delta\mathbf{q}^n = \frac{1}{3}\Delta\mathbf{q}^{n-1} - \frac{2}{3}\Delta t\mathbf{R}^n,$$

where I is identity matrix. The block-matrix system of algebraic equations was solved by the iterative Gauss-Seidel algorithm.

The algorithm and the computational program were verified by solving the task of flow around the wing profile, the results are presented in the study by Prykhodko *et al.,* [22].

3. Results

The results of numerical simulation of airflow around a pointed plate are presented in Figure 3 at zero angle of attack. The results are shown in the form of isolines of Mach number (iso-Mach contours) for different Mach numbers and different elongations.

From the data presented in Figure 3 it is seen that a vortex asymmetric structure appears behind the plate at subsonic velocities, the so-called Karman vortex street. As the velocity increases to transonic values, the aerodynamic trail stabilizes and the vortex system disappears. With increasing velocity, but at M <1, local supersonic zones begin to form in places of surface fracture. One of these local supersonic zones is formed at the place of transition from the smooth part to the wedge-shaped. Note that for a body of greater elongation, this area is more marked. With a further increase in velocity, this supersonic zone is gradually shifted to the nose part, where at M> 1 the attached shock wave is formed. Another inclined shock wave is formed on the trailing edge of the plate.

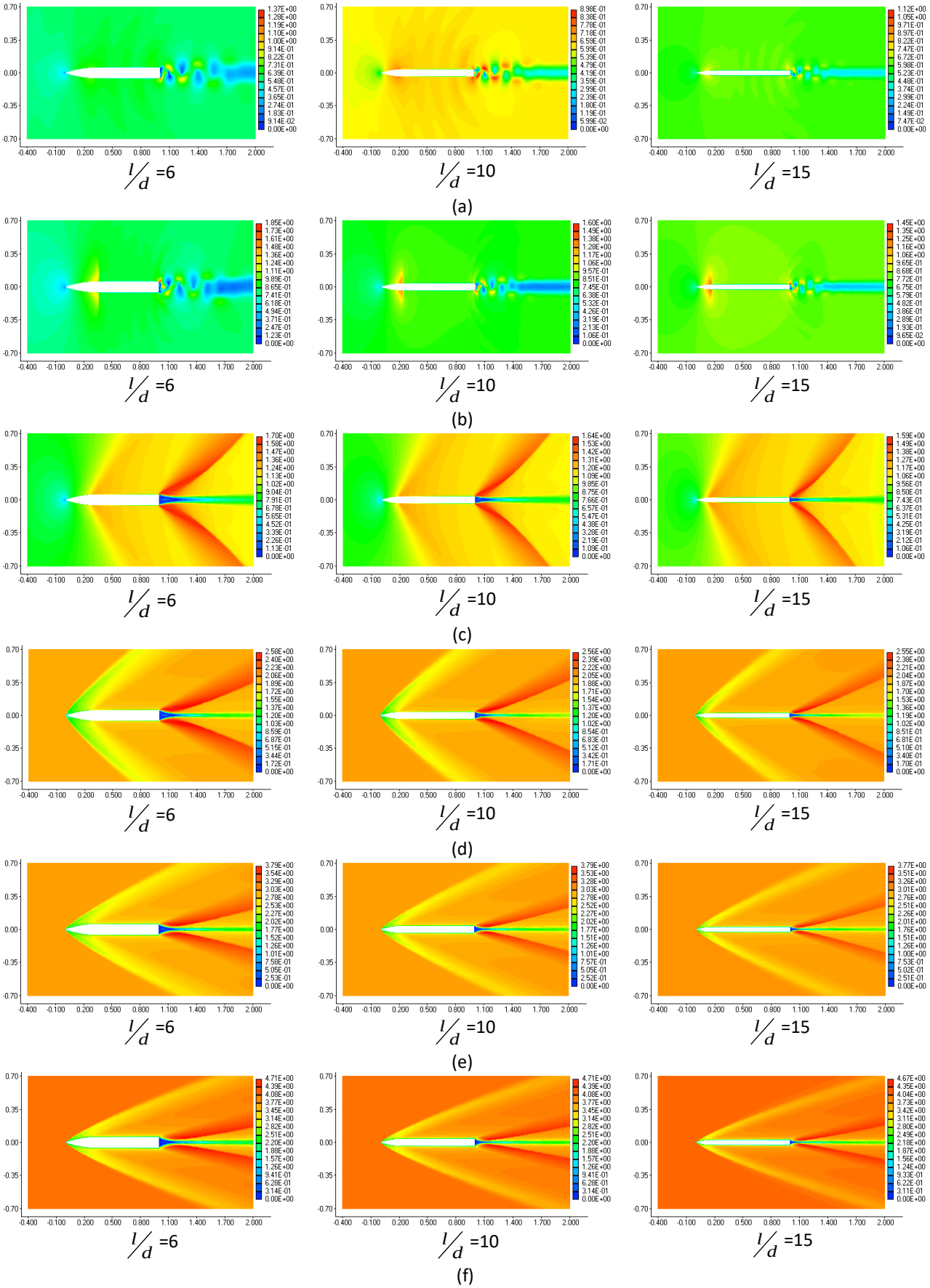

Fig. 3. Pattern of the flow around the pointed plate for different Mach numbers: (a) M = 0,6; (b) M = 0,8; (c) M = 1; (d) M = 2; (e) M = 3; (f) M = 4

Analysis of the aerodynamic flow pattern of plates of different elongation shows that with increasing ratio l/d the area of low supersonic velocities decreases in the bottom. It must also be noted that the increase in elongation leads to a slight decrease in the angle of inclination of the main inclined shock wave, which will mean less loss of mechanical energy of the flow and a decrease in impedance for bodies of greater elongation. The influence of Mach number and plate elongation on aerodynamic drag is presented in Figure 4.

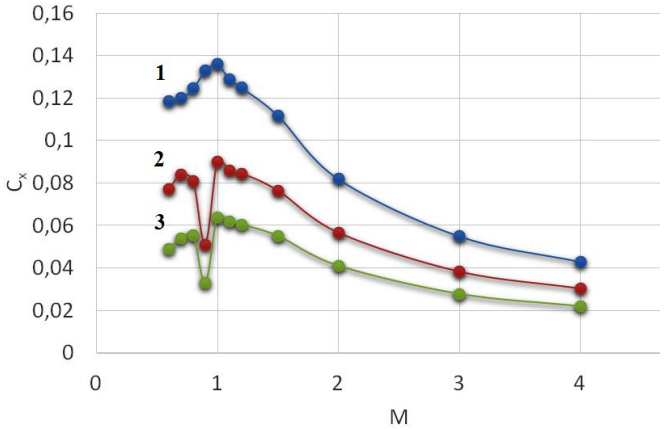

Fig. 4. Dependence of the drag coefficient on Mach number and the ratio *l/d*: 1 – 6; 2 – 10; 3 – 15

As can be seen from the obtained data, the drag coefficient is smaller for the bodies of greater elongation for the whole range of Mach numbers. Despite the fact that increasing the elongation of the body leads to an increase in frictional air drag, total drag coefficient decreases due to decrease of other components of the drag force: body base drag and shock wave drag, and due to the transfer of boundary-layer flow separation zone. The maximum frictional air drag is observed at M = 1. Numerical experiments showed a sharp drop in drag coefficient of a thick pointed plate in the area of transonic velocities (M≈0,9) at large elongations l/d = 10 and l/d = 15. This effect needs experimental confirmation. Figure 5 shows the dependences of drag coefficient on elongation at different Mach numbers. The data are shown without taking into account the transonic area, where, as shown above, the behavior of drag coefficient is abnormal.

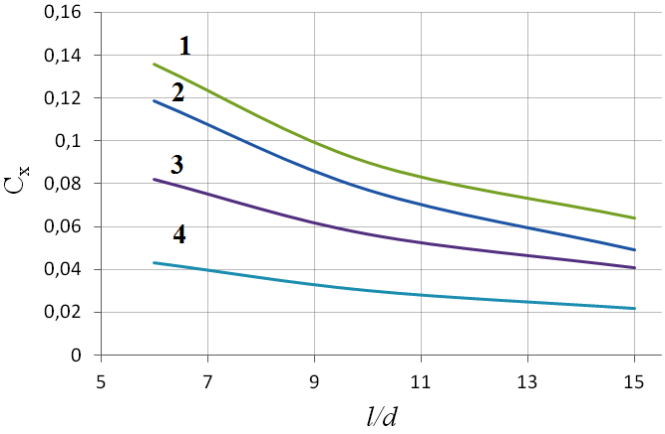

Fig. 5. Dependence of the plate coefficient C_x on the elongation: M=0.6; M=1; M=2; M=4

As can be seen from Figure 5, for the considered Mach numbers, the drag coefficient increases by 2-2,4 times with elongation decreasing from l/d = 15 to l/d = 6. Changing the drag coefficient may cause the loss of aerodynamic stability of the body, which must be taken into account when designing the aircraft. Also, a change in drag coefficient means a change in the ballistic coefficient of the body, which is one of the determining parameters for a flight path computation of the object.

4. Conclusions

The proposed model and method of numerical analysis allowed to study the aerodynamics of a pointed thick plate in subsonic and supersonic gas flow conditions. The obtained results of numerical simulations show that the elongation of the plate significantly affects the coefficient of aerodynamic drag during subsonic and supersonic flow. As the elongation decreases, the drag increases, so as the ratio decreases from l/d = 15 to l/d = 6, the drag increases up to 2,4 times depending on Mach number. The effect of a sharp decrease in the drag of the pointed plate is found at the transonic area. The simulation results are of interest to developers of new aircraft, in which it is possible to change the elongation of the structure during the flight.

Acknowledgement

The work was performed within the frame of project "Substantiation of design-ballistic parameters of ultralight launch vehicles with polymer bodies taking into account aerodynamic, thermophysical affects" № 0121U109770, funded by the Ministry of Education and Science of Ukraine.

References

[1] Moran, Jack. *An introduction to theoretical and computational aerodynamics*. Courier Corporation, 2003.
[2] Khan, Sher Afghan, Abdul Aabid, Imran Mokashi, Abdulrahman Abdullah Al-Robaian, and Ali Sulaiman Alsagri. "Optimization of two-dimensional wedge flow field at supersonic Mach number." *CFD Letters* 11, no. 5 (2019): 80-97.
[3] Aabid, Abdul, Azmil Afifi, Fharukh Ahmed Ghasi Mehaboob Ali, Mohammad Nishat Akhtar, and Sher Afghan Khan. "CFD analysis of splitter plate on bluff body." *CFD Letters* 11, no. 11 (2019): 25-38.
[4] Traub, Lance W. "Sweep and Thickness Effects on Flat-Plate Wings at Low Reynolds Number." *Journal of Aircraft* 58, no. 6 (2021): 1416-1423. https://doi.org/10.2514/1.C036445
[5] Yusof, Nur Syamila, Siti Khuzaimah Soid, Mohd Rijal Illias, Ahmad Sukri Abd Aziz, and Nor Ain Azeany Mohd Nasir. "Radiative Boundary Layer Flow of Casson Fluid Over an Exponentially Permeable Slippery Riga Plate with Viscous Dissipation." *Journal of Advanced Research in Applied Sciences and Engineering Technology* 21, no. 1 (2020): 41-51. https://doi.org/10.37934/araset.21.1.4151
[6] Seshadri, Pradeep Kumar, and Ashoke De. "Investigation of shock wave interactions involving stationary and moving wedges." *Physics of Fluids* 32, no. 9 (2020): 096110. https://doi.org/10.1063/5.0020365
[7] James, J. K., and H. D. Kim. "Flow Characteristics of a Mixed Compression Hypersonic Intake." *Journal of Applied Fluid Mechanics* 15, no. 3 (2022): 633-644. https://doi.org/10.47176/JAFM.15.03.33282
[8] Zuan, A. M. S., A. Ruwaida, S. Syahrullail, and M. N. Musa. "The Effect of Adding Diffuser by Experimental." *Journal of Advanced Research in Applied Mechanics* 14, no. 1 (2015): 18-24.
[9] Dai, Pei, Binbin Yan, Wei Huang, Yifei Zhen, Mingang Wang, and Shuangxi Liu. "Design and aerodynamic performance analysis of a variable-sweep-wing morphing waverider." *Aerospace Science and Technology* 98 (2020): 105703. https://doi.org/10.1016/j.ast.2020.105703
[10] Prikhod'ko, A. A., S. V. Alekseenko, and V. V. Chmovzh. "Experimental Investigation of the Influence of the Shape of Ice Outgrowths on the Aerodynamic Characteristics of the Wing." *Journal of Engineering Physics and Thermophysics* 92, no. 2 (2019): 486-492. https://doi.org/10.1007/s10891-019-01955-1
[11] Niknahad, Ali, and Abdolamir Bak Khoshnevis. "Numerical study and comparison of turbulent parameters of simple, triangular, and circular vortex generators equipped airfoil model." *Journal of Advanced Research in Numerical Heat Transfer* 8, no. 1 (2022): 1-18.

[12] Yemets, Vitaly, Mykola Dron', and Anatoly Pashkov. "Autophage engines: Method to preset gravity load of solid rockets." *Journal of Spacecraft and Rockets* 57, no. 2 (2020): 309-318. https://doi.org/10.2514/1.A34597
[13] Dreus, Andrii, Vitaly Yemets, Mykola Dron, Mykhailo Yemets, and Aleksandr Golubek. "A simulation of the thermal environment of a plastic body of a new type of launch vehicle at the atmospheric phase of the trajectory." *Aircraft Engineering and Aerospace Technology* 94, no. 4 (2022): 505-514. https://doi.org/10.1108/AEAT-04-2021-0100
[14] Dron, M., A. Dreus, Y. E. V. Abramovsky, and A. Golubek. "Investigation of aerodynamic heating of space debris object at reentry to earth atmosphere." In *Proceedings of the International Astronautical Congress*, IAC. 2018.
[15] Golubek, Aleksandr, Mykola Dron, Ludmila Dubovik, Andrii Dreus, Oleksii Kulyk, and Petro Khorolskiy. "Development of the Combined Method to De-Orbit Space Objects Using an Electric Rocket Propulsion System." *Eastern-European Journal of Enterprise Technologies* 4, no. 5-106 (2020): 78-87. https://doi.org/10.15587/1729-4061.2020.210378
[16] Petrov, K. P. "Aerodynamics of aircraft elements." *Mashinostroenie, Moscow* (1985).
[17] Yemets, V., M. Dron, A. Pashkov, A. Dreus, Y. Kositsyna, M. Yemets, L. Dubovyk, O. Kostritsyn, and P. Zhuravel. "Method to preset G-load profile of launch vehicles." In *Proceedings of the International Astronautical Congress*, IAC. 2020.
[18] Khan, Sher Afghan, Musavir Bashir, Maughal Ahmed Ali Baig, and Fharukh Ahmed Ghasi Mehaboob Ali. "Comparing the effect of different turbulence models on the CFD predictions of NACA0018 airfoil aerodynamics." *CFD Letters* 12, no. 3 (2020): 1-10. https://doi.org/10.37934/cfdl.12.3.110
[19] Spalart, Philippe, and Steven Allmaras. "A one-equation turbulence model for aerodynamic flows." In *30th Aerospace Sciences Meeting and Exhibit*, p. 439. 1992. https://doi.org/10.2514/6.1992-439
[20] Peyret, Roger, and Thomas D. Taylor. *Computational methods for fluid flow*. Springer Science & Business Media, 1982. https://doi.org/10.1007/978-3-642-85952-6
[21] Kim, Sung-soo, Chongam Kim, Oh-Hyun Rho, and Seung Kyu Hong. "Cures for the shock instability: development of a shock-stable Roe scheme." *Journal of Computational Physics* 185, no. 2 (2003): 342-374. https://doi.org/10.1016/S0021-9991(02)00037-2
[22] Prykhodko, A. A., S. V. Alekseyenko, and V. V. Prikhodko. "Numerical investigation of the influence of horn ice formation on airfoils aerodynamic performances." *International Journal of Fluid Mechanics Research* 46, no. 6 (2019): 499-508. https://doi.org/10.1615/InterJFluidMechRes.2019026024